

One-dimensional quadratic walking solitons

R. Schiek, Y. Baek, and G. I. Stegeman

Center for Research and Education in Optics and Lasers, University of Central Florida,
4000 Central Florida Boulevard, Orlando, Florida 32816-2700

W. Sohler

Angewandte Physik, Universität Paderborn, Warburger Strasse 100, D-33098 Paderborn, Germany

Received October 16, 1998

The properties of one-dimensional quadratic walking solitons were investigated in planar lithium niobate waveguides near the type I phase-matching condition for second-harmonic generation. Wave propagation was studied under different conditions of phase matching, walk-off angle, and incident fundamental power. © 1999 Optical Society of America

OCIS codes: 190.4390, 190.4160, 130.3730.

Quadratic solitons were observed a few years ago during second-harmonic generation in both bulk crystals (two-dimensional) and planar waveguides (one-dimensional).^{1,2} They consist of strongly coupled fundamental (FUND) and second-harmonic (SH) fields that propagate locked together in space without diffraction. For propagation that is not parallel to the principal axis of birefringent crystals, the propagation direction of the evolving soliton from a given input field depends on the input power and the wave-vector mismatch. This property was used in subsequent research to demonstrate all-optical switching and beam scanning with two-dimensional solitons.³ The principal physical concepts involved in this nonlinear beam steering were investigated later theoretically for one-dimensional solitons.^{4,5} There the term “walking soliton” was introduced because these solitons walked away from the input direction of the incident FUND.⁴ In this Letter we report investigations of the properties of one-dimensional quadratic walking solitons in type I SHG under conditions in which we tuned the soliton walk-off from zero to a finite value by varying the propagation angle from the crystal axis, the incident power, and the wave-vector mismatch.

The walking soliton fields are described by the eigenfunctions of a nonlinear eigenvalue problem that evolves from the coupled-mode equations for the spatial spectral components of the interacting beams^{2,6} when the derivatives in the propagation direction are fixed. The intensity of the FUND and the SH of a walking soliton calculated from a typical eigenfunction for off-axis propagation are shown in Fig. 1. The phase tilt of the FUND across the transverse direction of the beam depends strongly on the power ratio between the SH and FUND and the wave-vector mismatch. This soliton would propagate exactly in the propagation direction tilted from the principal axis by α for which the eigenvalue problem was solved. However, because a launching beam usually has no phase tilt across its transverse dimension such an input would launch not the calculated eigensolution but a slightly different one propagating in a slightly different direction, so the input beam's phase front would fit the phase front of the eigenfunction that propagates in the new direction. This direction depends on the transverse phase tilt

of the eigenfunction, which in turn is power and wave-vector dependent. Therefore we have a kind of nonlinear refractive effect in the launching of a walking soliton that induces the walking. This behavior is illustrated in Fig. 2 with a simulation of the evolution of a walking soliton from an input field that propagates at low power along $y = 0$, which corresponds to a direction tilted $\alpha = -3.25^\circ$ away from the principal crystal axis. In the soliton formation process near the input, the SH part of the soliton is generated and stays as the bound SH in the soliton. Generated also is a free SH, which diffracts and radiates with its walk-off angle. The walking soliton direction is always found in the region between the FUND beam direction for low power and the walk-off direction of the free SH. With increasing bound SH in the soliton the soliton direction shifts toward the walk-off direction of the radiated SH.

The experiments were performed in an x -propagating $L = 47$ -mm-long LiNbO₃ crystal into which a slab waveguide was fabricated by Ti indiffusion along the crystallographic y axis. For the type I SH generation geometry used, the dominant electric field of the FUND TM₀ mode was y polarized and the SH TE₁ mode was polarized along the z axis. The laser used was a Nd:YAG operating in Q -switched and mode-locked mode at $\lambda = 1.32 \mu\text{m}$ with 90-ps pulses. As in our previous experiments on soliton generation

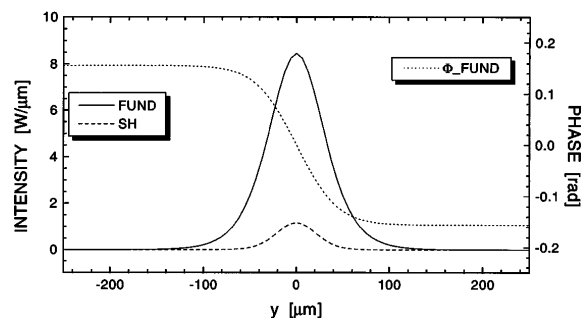


Fig. 1. FUND and SH components of a walking soliton in type I SHG in a uniform lossless LiNbO₃ film waveguide on a y -cut crystal propagating at an angle of $\alpha = -3.25^\circ$ from the crystal x axis. The phase variation across the FUND beam profile is a key characteristic of the walking-soliton temperature, $\vartheta = 333.1^\circ\text{C}$.

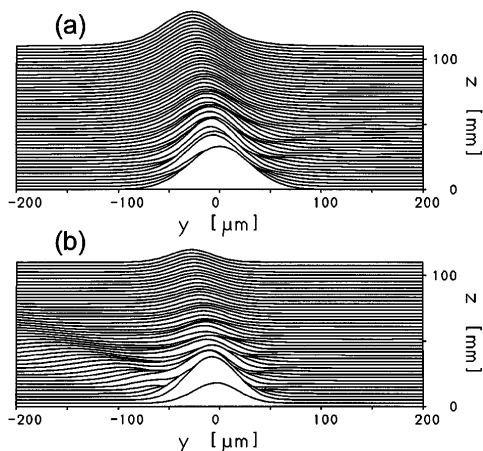


Fig. 2. Formation of a walking soliton in a uniform lossless LiNbO₃ film waveguide: (a) FUND beam, (b) SH beam. Only the FUND beam with a power of 900 W was launched in a direction tilted $\alpha = -3.25^\circ$ from the x crystal axis. At low power the FUND beam diffracts to a width of $400 \mu\text{m}$ at $z = 110 \text{ mm}$ with its center staying at $y = 0$, $\vartheta = 333.1^\circ \text{C}$.

in this sample, only the FUND beam with a full width at half-maximum of $70 \mu\text{m}$ was input, and the SH required for quadratic soliton generation was generated on propagation into the waveguide.² Temperature-tuned phase matching at this wavelength required operation at temperatures near 335°C , and hence an oven was used to house the crystal. As was discussed in detail before,^{2,6} this process leads to a nonuniform temperature (and therefore to a wave-vector mismatch) distribution along the crystal, with advantageous consequences for the formation of solitons with only FUND input.⁷ We performed the experiments by rotating the LiNbO₃ waveguide about the y axis to facilitate propagation off the principal x axis. Because the total width of the waveguide was only 5 mm , the maximum off-axis angle that could conveniently be launched was 4° . The FUND and the SH beams at the output were observed with a vidicon camera. The theoretical data for comparison with experiment were calculated with all the experimental details taken into account.

Figure 3 shows the FUND depletion curves for several off-axis propagation angles α . Because of the negative birefringence of LiNbO₃ the phase-matching temperature decreases with increasing off-axis propagation. At the largest phase-matching temperature the adjustment with $\alpha = 0^\circ$ was found where the FUND and the SH propagated exactly along the x axis. As the crystal was turned, the low-power FUND propagated inside the crystal in a direction tilted by $\alpha \neq 0$ from the x axis. The centers of the diffracted output beams of both the observed FUND ($180 \mu\text{m}$ wide) and the SH separated increasingly with increasing α because of the walk-off of the SH.

We easily generated quadratic solitons in the temperature region below phase matching by increasing the input FUND peak power to larger than $P_F \approx 1500 \text{ W}$, with the correct value depending on beam width and temperature. When the soliton had formed, both the FUND and the SH of the soliton

merged at the output face, shifted to an intermediate point between the low-power outputs of the SH and FUND beams. Representative results of measurements of the output beams for $\alpha = -3.25^\circ$ at a temperature of $\vartheta = 332.8^\circ \text{C}$ are shown in Fig. 4. The

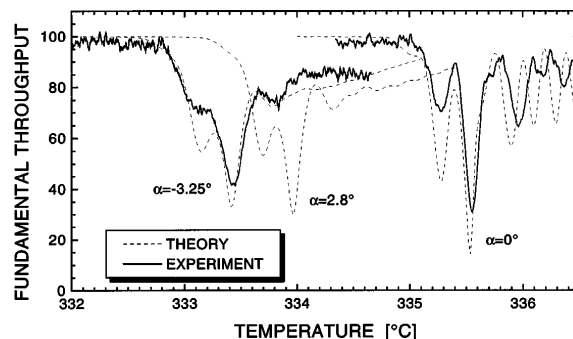


Fig. 3. Temperature-tuned FUND depletion curves for three off-axis launching angles. The FUND input peak power of $P_F = 375 \text{ W}$ is below the power for soliton generation in the low-depletion regime.

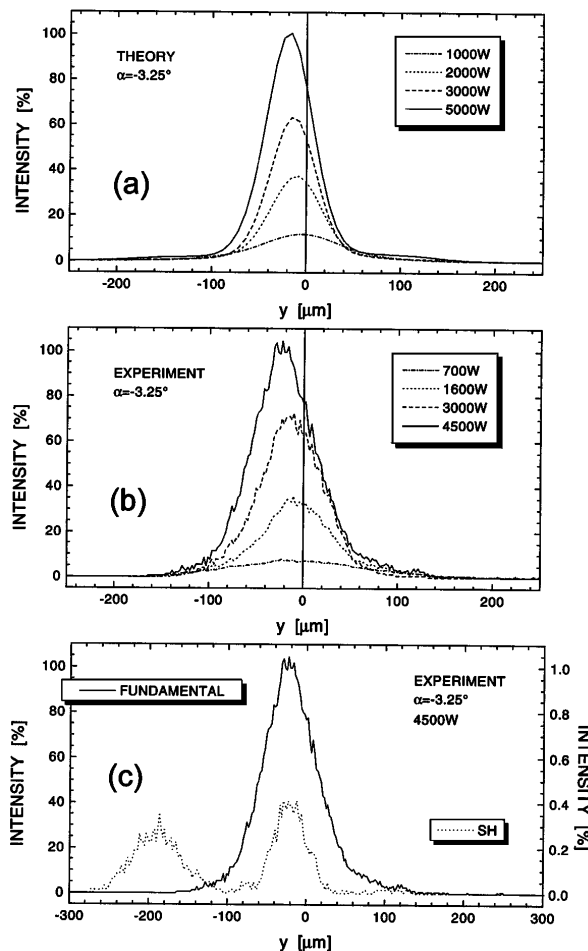


Fig. 4. Power dependence of the soliton beam's location at the outcoupling surface of the waveguide for an off-axis angle of $\alpha = -3.25^\circ$ at a temperature of $\vartheta = 332.8^\circ \text{C}$: (a) FUND beam, theory, (b) FUND beam, experiment, (c) FUND and SH. The 0 position corresponds to the output position of the low-power diffracted FUND beam. The intensities are normalized to the maximum FUND intensity.

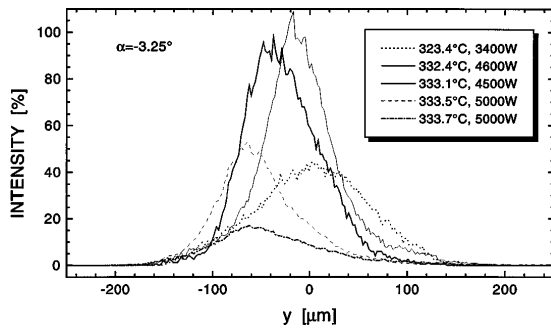


Fig. 5. Temperature dependence of the soliton beam's location at the outcoupling surface of the waveguide; $\alpha = -3.25^\circ$, $P_F \approx 4500$ W.

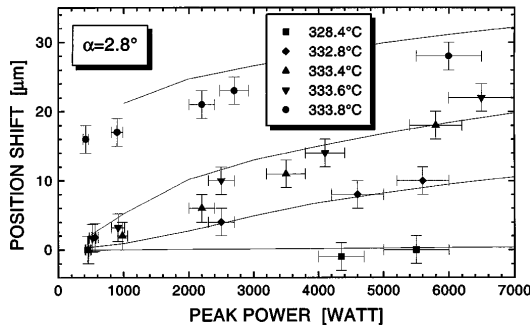


Fig. 6. Power dependence of the shifted beam's location for five temperatures, i.e., different strong cascaded nonlinearities. Solid curves, simulation; symbols, experiment.

soliton width, the power ratio between the SH and the FUND component P_{SH}/P_F , and the transverse phase distribution of the soliton fields vary with FUND input power. We cannot observe a significant narrowing of the output beams below $70 \mu\text{m}$ for increasing power because narrower solitons than $70 \mu\text{m}$ already diffract in the colder oven end zone where the cascaded nonlinearity is no longer sufficient to counteract diffraction. However, in the 35-mm-long oven center (with a more nearly uniform wave-vector mismatch) the soliton with the higher power has a larger ratio P_{SH}/P_F , yielding a larger transverse phase tilt of the FUND. The resultant shift of the soliton position toward the walked-off SH position with increasing power is clearly observable in Figs. 4(a) and 4(b). In Fig. 4(c) the SH and the FUND at the output are compared. The narrow bound SH soliton part is distinguishable from the diffracted and walked-off free SH, which was generated in the soliton formation process near the input. The measured beam profiles and positions fit the simulation results very well. For this large a wave-vector mismatch of $\Delta\beta L = 10\pi$ at

$\vartheta = 332.8^\circ\text{C}$ the SH part of the soliton carried less than 20% of the total power for all our input powers, and the depletion of the FUND is not significant.

Figure 5 illustrates the shift in the soliton location when the temperature and therefore the wave-vector mismatch are varied from 125π to -1.7π with the FUND input power kept constant. The closer the temperature approaches the phase-matching temperature, the larger is the SH component of the soliton and the more the propagation direction of the walking soliton shifts toward the walked-off SH. In Fig. 5 the depletion of the FUND for temperatures $\vartheta > 333.3^\circ\text{C}$ ($\Delta\beta L < 3\pi$) is shown to be significant, and within our short sample the soliton formation process with the consequent generation of the SH part from the FUND input has not reached steady state so the beams still oscillate and are not yet stationary solitons.⁶

The measurements were done for several angles α . The positive shift in the beam location for $\alpha = 2.8^\circ$ for various power and wave-vector mismatch values (i.e., different temperatures) is summarized in Fig. 6. The measured values agree well with the simulation results, which are plotted as solid curves.

In summary, the mutual locking between the FUND and the SH to form a quadratic soliton produces a nonlinear translation of the output position of the solitary wave when the FUND input angle is detuned from propagation along a principal crystal axis under a variety of phase-mismatch and power conditions. It was verified that walking solitons are generated in a number of different circumstances.

This research was supported by the National Science Foundation and the U.S. Air Force Office of Scientific Research. R. Schiek's e-mail address is schiek@tep.e-technik.tu-muenchen.de.

References

1. W. E. Torruellas, Z. Wang, D. J. Hagan, E. W. Van Stryland, G. I. Stegeman, L. Torner, and C. R. Menyuk, *Phys. Rev. Lett.* **74**, 5036 (1995).
2. R. Schiek, Y. Baek, and G. I. Stegeman, *Phys. Rev. E* **53**, 1138 (1996).
3. W. E. Torruellas, G. Assanto, B. L. Lawrence, R. A. Fuerst, and G. I. Stegeman, *Appl. Phys. Lett.* **68**, 1449 (1996).
4. L. Torner, D. Mazilu, and D. Mihalache, *Phys. Rev. Lett.* **77**, 2455 (1996).
5. C. Etrich, U. Peschel, F. Lederer, and B. Malomed, *Phys. Rev. E* **55**, 6155 (1997).
6. R. Schiek, Y. Baek, G. I. Stegeman, and W. Sohler, *Opt. Quantum Electron.* (to be published).
7. L. Torner, C. B. Clausen, and M. M. Fejer, *Opt. Lett.* **23**, 903 (1998).